CALCULATION AND MEASUREMENT OF THE INFLUENCE OF FLOW PARAMETERS ON ROTORDYNAMIC COEFFICIENTS IN LABYRINTH SEALS

K. Kwanka, W. Ortinger, and J. Steckel
Lehrstuhl Thermische Kraftanlagen
Technische Universität München
München, Germany

Abstract

First experimental investigations performed on a new test rig are presented. For a staggered labyrinth seal with fourteen cavities the stiffness coefficient and the leakage flow are measured. The experimental results are compared to calculated results which are obtained by a one-volume bulk-flow theory. A perturbation analysis is made for seven terms. It is found out that the friction factors have great impact on the dynamic coefficients. They are obtained by turbulent flow computation by a finite-volume model with the Reynolds-equations used as basic equations.

Nomenclature

C, E, K	Damping, inertia, stiffness coefficients
F	Force
H	Labyrinth height
U	Part of cavity perimeter
c_f	Friction factor
$c_{u,}$ c_{ax}	Circumferential velocity, axial velocity
e	Eccentricity
f	Cross-sectional area of cavity
$\dot{m}$	Mass flow related to circumference
l	Length of cavity
n	Rotating speed
p	Pressure
R_R	Radius of rotor
δ	Radial clearance
φ	Peripheral angle
κ	Isentropic coefficient
λ	Friction factor
μ	Flow coefficient, dynamic viscosity
τ	Shear stress
$\Psi, \xi, \Lambda, \Xi, \eta, \zeta, \tilde{n}$	Perturbation terms
ω	Angular velocity
ρ	Density

Introduction

Despite the numerous efforts in the past, there still remain some open questions in understanding tip-clearance excitation and, as a consequence, a lack in modelling and predicting forces and coefficients induced by labyrinth flow. The efforts to increase the efficiency and to minimize the specific costs or the specific weight of a rotor-casing configuration often lead to parameters which are in some cases very close to the stability margin. Beyond the stability limit the rotational energy which is transferred to the rotor bending exceeds the damping that dissipates this energy. As a consequence, self-excited vibration mechanisms impede the scheduled operation regime of the turbomachine. In addition to the labyrinth seal forces several other mechanisms (e.g. oil whip) act on the rotor and an amplification of the excitation may occur [5].

The labyrinth seal forces are usually described in a linearized formulation for small deflections out of the centered position by using dynamic coefficients. These are stiffness, damping and inertia coefficients.

$$\vec{F} = -\begin{pmatrix} K_{xx} & K_{xy} \\ -K_{yx} & K_{yy} \end{pmatrix}\begin{pmatrix} x \\ y \end{pmatrix} - \begin{pmatrix} C_{xx} & C_{xy} \\ -C_{yx} & C_{yy} \end{pmatrix}\begin{pmatrix} \dot{x} \\ \dot{y} \end{pmatrix} - \begin{pmatrix} E_{xx} & E_{xy} \\ -E_{yx} & E_{yy} \end{pmatrix}\begin{pmatrix} \ddot{x} \\ \ddot{y} \end{pmatrix} \qquad (1)$$

Many investigations were performed to estimate the dynamic coefficients on several seal geometries. In the experimental field two procedures are frequently used. First, static measurements were made [4, 2,12] which allow the determination of the direct and cross-coupled stiffness coefficients of the labyrinth seal. Second, dynamic measurements [2, 7], which were carried out to identify the other coefficients in eq. (1).

The experimental results can be used for verification of the various theoretical approaches. The computational effort is low when a bulk-flow theory - either a one-, two- or three-volume model [1, 3, 8]- is used. An increased amount of computational time is needed if the seal geometry is discretized by a grid, and if the local variables are calculated by the finite-difference or the finite-volume method [9]. The forces acting on the rotor are obtained by a final integration.

In this paper a staggered labyrinth seal is investigated. Only few experimental results are published for this geometry in comparison to others. With the help of the static identification method a maximum accuracy for the measured stiffness coefficients is expected. In most cases these coefficients are of outstanding importance for the dynamic behaviour of the rotor.

The calculated results are obtained by a one-volume bulk-flow theory. It is found out that the bulk-flow theory in connection with the perturbation method is highly sensitive to friction factors. In this case they are calculated by means of turbulent flow computation. The Reynolds equations in cylindrical coordinates including the standard k-ε model give the velocity components and the turbulent values. A boundary-layer theory is applied and the friction factors are calculated depending on the axial and circumferential status of the flow.

Test Rig

The test rig is designed with the purpose to measure labyrinth flow induced radial forces on the eccentric rotor. In fig. 1a. a schematic representation of the test rig can be seen. Two identical grooved labyrinth seals with fourteen cavities each are located symmetrically to the inflow region. The inflow region is outlined in fig. 1b. The inlet swirl can be varied by the combination of radial and circumferential flow components.

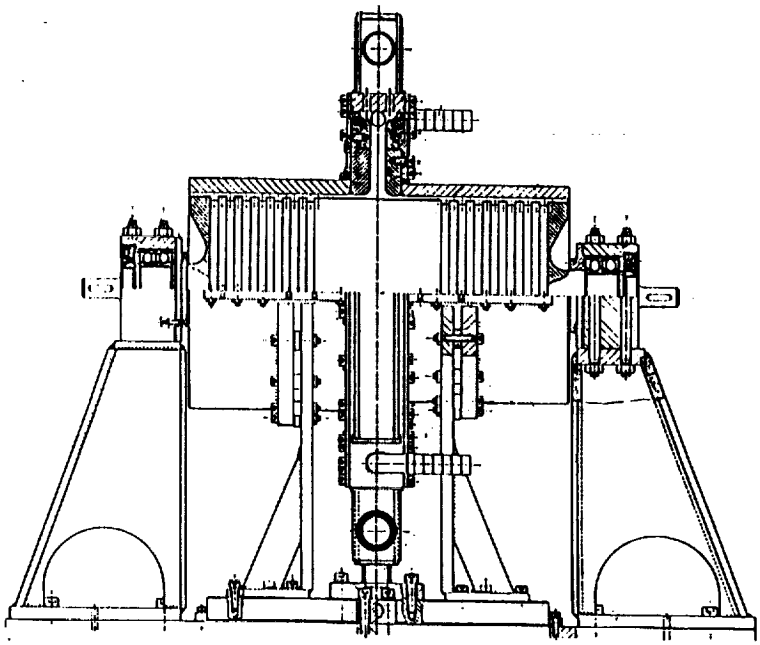

Fig. 1a. Schematic of the test rig

The geometric data of the staggered labyrinth are indicated in fig. 2. At the center position the gap between the rotor and the seal tips attached to the casing is 0.5 mm. The eccentricity can be adjusted in horizontal direction by moving the casing relative to the rotor.
One of the seals is used to measure the pressure distribution in circumferential direction and, as a consequence, the acting force in each cavity and on the whole rotor. Ten pressure lines are located in each cavity. This gives a total of some 160 data points per labyrinth seal unit. The pressure lines are connected to a multifunction pressure measurement rig. The flow field in the cavities and the inlet swirl is determined by using a probe which is located in the second labyrinth seal.

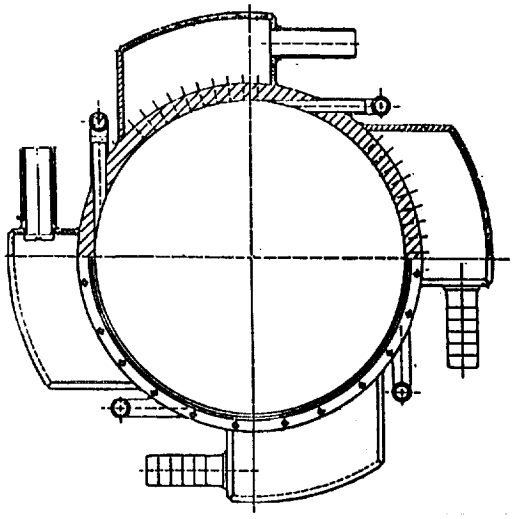

Fig. 1b. Inflow configuration of the test rig

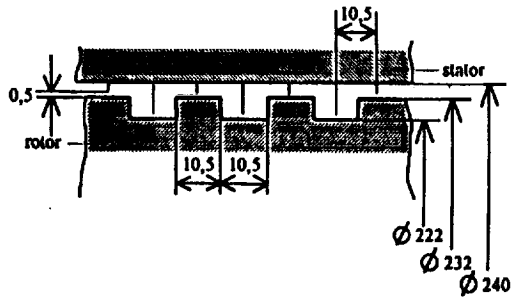

Fig. 2. Geometric data of the labyrinth (dimensions in mm)

Some test rig dimensions and experimental conditions are listed in table 1. The maximum preswirl velocity ($c_u \approx 22$ m/s) is reached when there is an inflow only via the tangential feeders. Due to the fact that the direction of the rotational speed can be changed the preswirl can be negative and positive. With high pressure differences on the labyrinth seal the critical pressure ratio prevailes on the last seal tip.

Table 1. Test rig dimensions and experimental conditions

Diameter (stator)	D [mm]	240
Length (seal)	L [mm]	150
Clearance (e=0)	d [mm]	0,5
Eccentricity	e [mm]	max. 0,4
Pressure difference	Δp [kPa]	max. 450
Rotating speed	n [rpm]	±8000

First measurements at the center position show that the pressure is declining in axial direction, alternately in big and small steps. Together with the geometry dependent flow area this causes a zigzag course of the flow coefficient (fig. 3), which is almost entirely independent on the rotational speed, inlet swirl and eccentricity. The mean value of the flow coefficient in the neutral position of the rotor is 0.69 and 0.675 when the eccentricity is 0.4 mm.

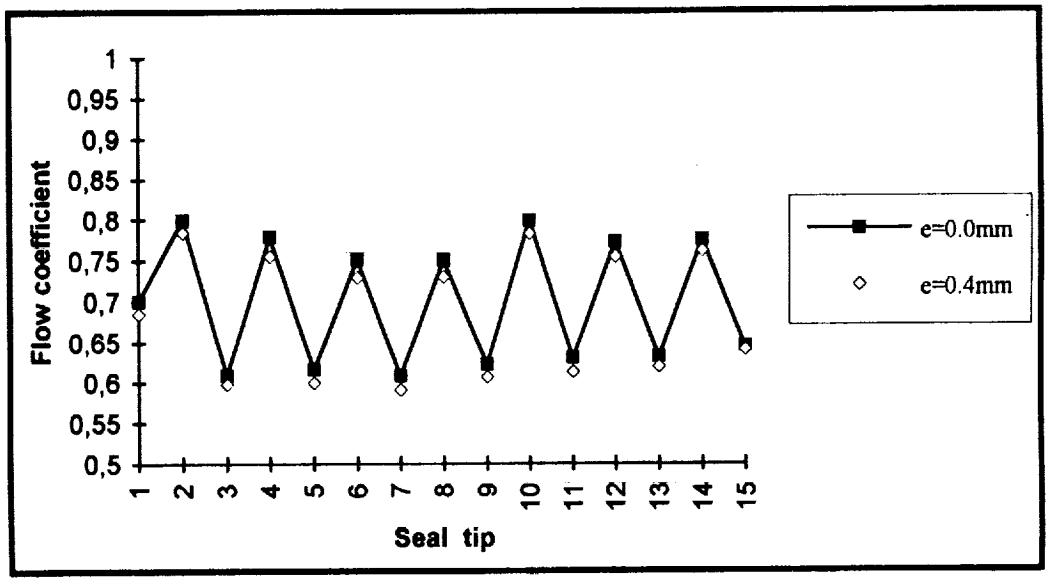

Fig. 3. Flow coefficient for centric and eccentric position of the rotor (Δp = 160000 Pa; n = 4000 rpm)

Considering the direction of displacement, the force acting on the rotor can be splitted in a restoring and a cross force. Despite the fact that the restoring force is conservative it has an influence on the critical speeds and the vibrational modes and thus on the stability. When the restoring force has a decentralized effect the bending modes are in general more deflected and more excited by cross forces, and the stability limit declines.

In center position of the rotor the circumferential pressure distribution in each cavity has shown that almost no resulting force is acting on the rotor and which means that the rotor is well manufactured and exactly alined. At the off-center position of the rotor the restoring force has a zigzag course like the flow coefficient (fig. 4). The resulting force for the whole labyrinth

is decenterizing for all parameters investigated. This behavior of the restoring force can be explained by the change of state of the throttled flow in the alternating large flow areas in the cavity and the small flow areas between the strips and rotor. Only in the gap behind the last seal tip the direction of the force is directed against the deflection as is normally expected for plain seals.

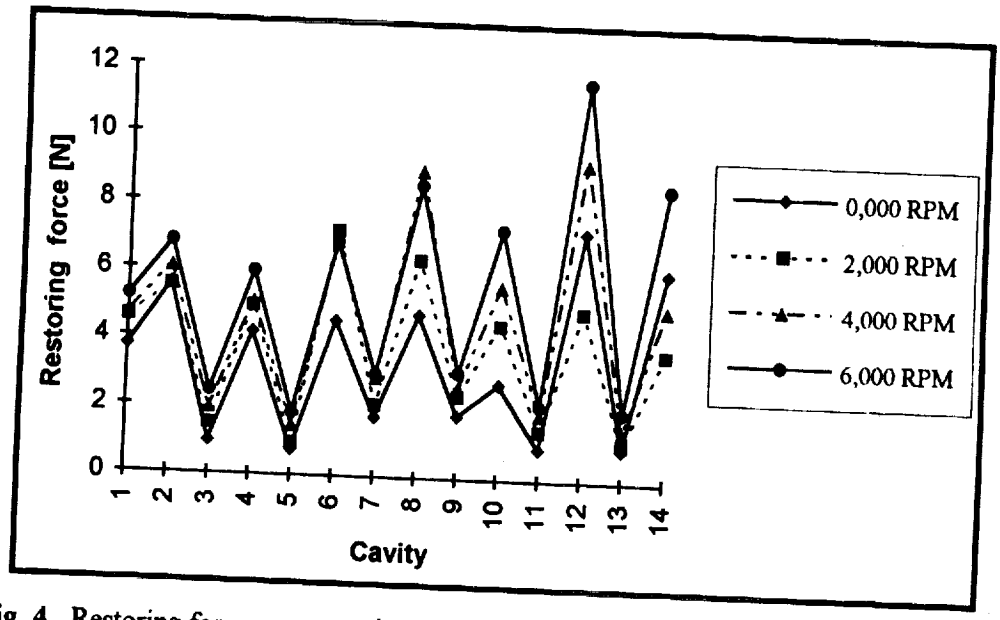

Fig. 4. Restoring force versus cavity in dependence of rotating speed ($\Delta p = 300000$ Pa; $e = 0.4$ mm; $c_u \approx 22$ m/s)

From a maximum in the first cavities the cross force declines towards the end of the labyrinth seal (fig. 5). The influence of the rotational speed on the restoring and the cross force is small. For all investigated parameters the restoring force was higher than the cross force.

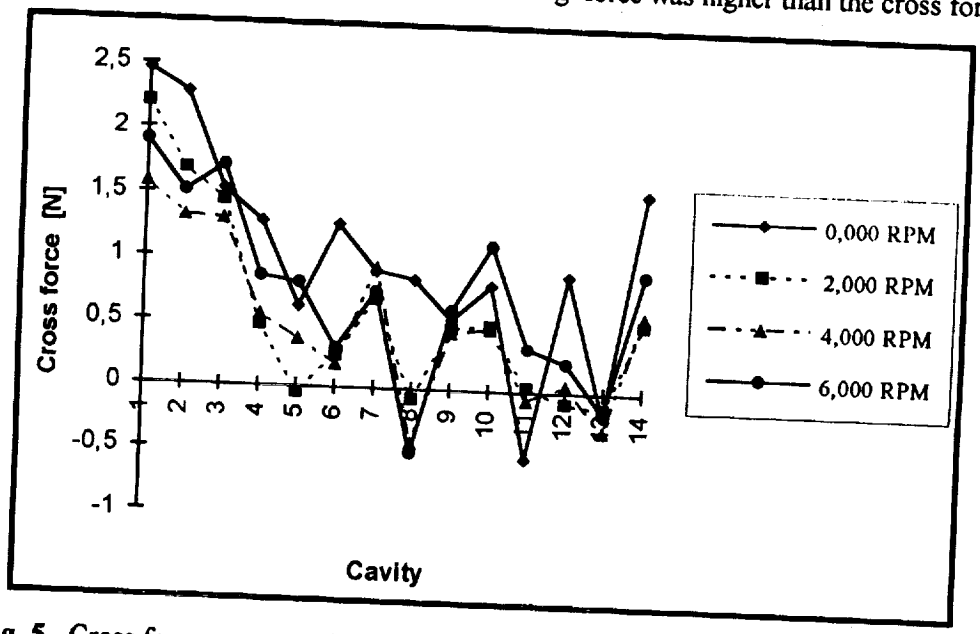

Fig. 5. Cross force versus cavity in dependence of rotating speed ($\Delta p = 300000$ Pa; $e = 0.4$ mm; $c_u \approx 22$ m/s)

The rotational speed and the entry swirl act together and influence the magnitude of the destabilizing force (fig. 6). When the direction of rotation and inlet swirl coincide then the cross force is smaller than in case of counteracting swirl and drag exerted by the rotating surface of the rotor to the flow. The influence of swirl exceeds the influence of rotation. Decisive for the magnitude of the cross force is the change of circumferential velocity and not the absolute value of this velocity. In case of conspiring swirl and drag the circumferencial velocity has the highest values but not the cross force.

Further details about the experimental investigations effected under consideration of numerous parameters are contained in [11].The circumferential velocity c_u in front of the seal is about 20 m/s for all investigations in this paper which are performed with swirl .

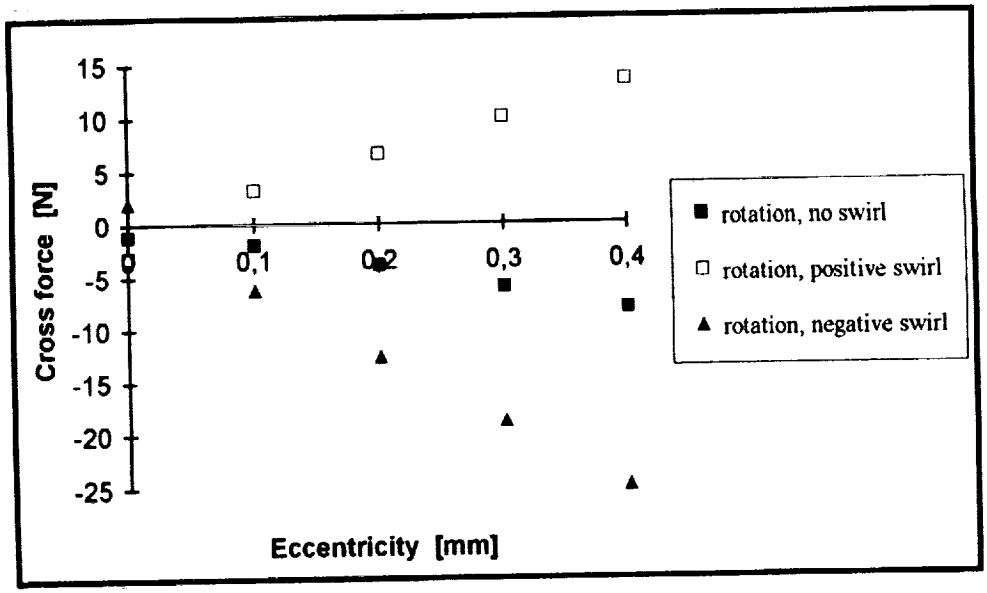

Fig. 6. Influence of entry swirl and rotating speed on the cross force (Δp = 460000 Pa; n = 4000 rpm)

Theoretical Treatment

With the help of a bulk-flow theory the circumferential pressure distribution due to the eccentric position of the rotor relative to the casing is obtained.

The governing equations are the following:

$$\dot{m}_i = \mu_i \delta_i \sqrt{p_{i-1}^2 - p_i^2}$$

$$\frac{\partial}{\partial t}(\rho_i f_i) + \frac{\partial}{R_R \partial \varphi}(\rho_i c_{ui} f_i) + \dot{m}_{i+1} - \dot{m}_i = 0$$

(2) - (5)

$$\frac{\partial c_{ui}}{\partial t} + c_{ui}\frac{\partial c_{ui}}{R_R \partial \varphi} + \dot{m}_i \frac{c_{ui} - c_{ui-1}}{\rho_i f_i} + \kappa_{Si} c_{ui}^2 - \kappa_{Ri}\left(R_R\omega - c_{ui}\right)^2 = -\frac{\partial p_i}{\rho_i R_R \partial \varphi}$$

$$\kappa_{Si} = \lambda_{Si}\frac{U_{Si}}{2f_i} sgn(c_{ui}) \quad ; \quad \kappa_{Ri} = \lambda_{Ri}\frac{U_{Ri}}{2f_i} sgn(R_R\omega - c_{ui})$$

This is the well-known set of partial differential equations. In order to find an analytical solution the differential equation system is linearized by splitting the main variables into an average value (for the centric position) and an additional value for the eccentric position. This perturbation method is applicated for eight terms.

$$\delta = \delta_*(1+\Psi) \qquad f = f_*(1+\Xi) \qquad \dot{m} = \dot{m}_*(1+\zeta)$$
$$p = p_*(1+\xi) \qquad c_u = c_{u*}(1+\eta) \qquad \mu = \mu_*(1+\tilde{n}) \qquad (6)(a\text{-}h)$$
$$\lambda_R = \lambda_{R*}(1+\Lambda_R) \qquad \lambda_S = \lambda_{S*}(1+\Lambda_S)$$

The most important ones are ξ for the pressure distribution and Λ_S, Λ_R for the friction factor.

Eqs. (6) are put in eqs. (2) - (5) and an exponential formulation for the perturbation term leads to the cross force acting on the rotor of the labyrinth seal.

$$F = -R_R l\, p_* \int_0^{2\pi} \xi \sin\varphi d\varphi \qquad (7)$$

With the help of this perturbation method it is possible to calculate the forces in a first step and, in a second step, to obtain the dynamic coefficients of the seal. Details of the calculation method can be seen in [1].

The value of the cross force is influenced by two factors. First, by the difference of the circumferential velocity from chamber to chamber. This leads to methods to control the swirl, for example swirl-brakes or helically grooved seals, a well-known and often discussed phenomenon.

Second, a great influence of the cross forces on the friction factor is found. This can be seen in figure 7. For the given labyrinth geometry in the test rig a great variety of results for the cross forces is obtained by the application of several friction factors for labyrinth seals.

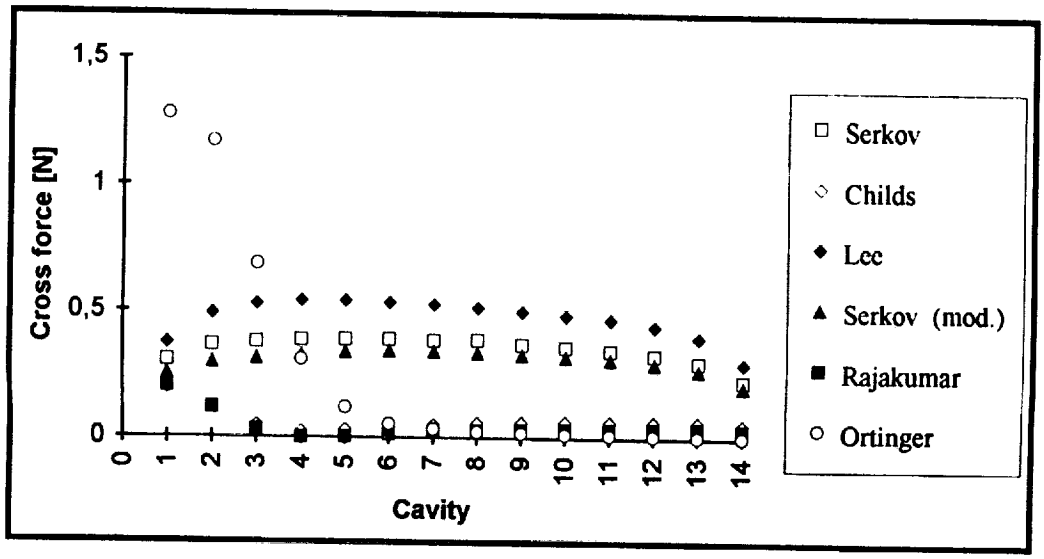

Fig. 7. Cross force in dependence on different methods to calculate the friction factor (Δp = 80000 Pa; n = 4000 rpm)

For the following calculations the friction factor is obtained by computing the turbulent flow field in the labyrinth seal with the Reynolds equations in connection with a k-ε turbulence model. The circumferential velocity near the wall is determined and a theory for the computation of the friction factor is applied.

$$c_f = \frac{\tau_W}{0.5\rho c_u} \qquad \lambda = 4c_f \tag{8}$$

For the shear stress on the labyrinth wall the following formulation is found:

$$\tau_W = \rho u_\tau^2 \tag{9}$$

where the shear stress velocity is dependent on the region where the calculated velocity occurs, i.e. either in the viscous sublayer or the full turbulent layer. Details can be seen in [10].

This theory leads to the friction factor of the seal. The Reynolds number is defined

$$\mathrm{Re} = \frac{\rho c_{ax} H}{2\mu} \tag{10}$$

Results of the calculated friction factor in relation to other methods can be seen in fig. 8.

For all the methods there can be observed a tendency of decreasing friction factors with increasing Reynolds numbers. For the calculated method the friction factor reaches an asymptotic value, whereas in the other cases the factors are still decreasing.

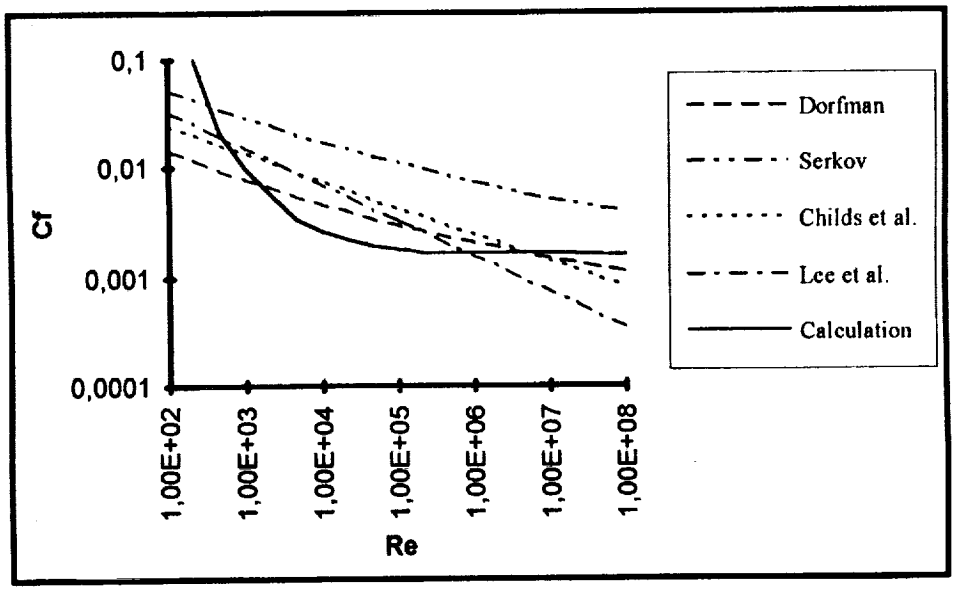

Fig. 8. Comparison of friction factors obtained by various methods and authors.

Comparison between Theory and Experiment

The cross coupled stiffness is an important input value for calculations of the rotordynamic stability limit. For three differencies of inlet and outlet pressure maximum preswirl and constant rotating speed the calculated results are compared to experimental results (fig. 9). The calculated results are obtained by the bulk-flow theory presented before including the friction factors contained in fig. 8.

The calculation exceeds slightly the experiment whereas the tendency is in good agreement. The almost proportional increase of the calculated cross force with the inlet-outlet pressure difference cannot be confirmed totally by experiment. The measured cross force is about linear to eccentricity.

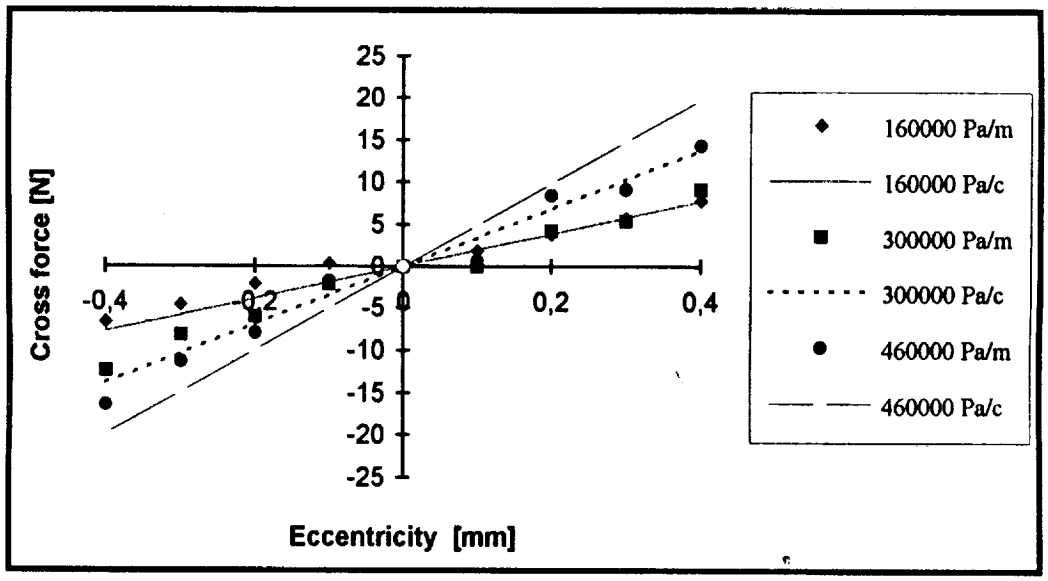

Fig. 9. Comparison of calculation and experiment in dependence of the pressure difference (n = 6000 rpm; m - measurement, c -calculation)

Conclusions

Measured normal and cross forces for a fourteen cavity staggered labyrinth are presented. The forces are obtained by the circumferential pressure distribution in each cavity when the rotor is in an eccentric position relative to the casing. The influence of inlet swirl, pressure ratio and rotor speed has been investigated.

The restoring force acts in direction of eccentricity and can decrease indirectly the stability limit. The cross force is linear to eccentricity and increases with the pressure ratio. Despite the fact that the length of the seal is large the effect of inlet swirl has a higher effect than the rotating speed. The absolute value of circumferential velocity is not decisive for the magnitude of the cross force which, is the highest in the first cavities.

The calculation of the labyrinth forces is very sensitive to friction factors. When the friction factors, which are obtained by turbulent flow computation are used as input quantities in a bulk-flow theory calculation the agreement with experimental data is fairly good.

References

[1] Baumgartner M.: *Evaluation of Exciting Forces in Turbomachinery Induced by Flow in Labyrinth Seals.* ASME Conf. on Mech. Vib. and Noise, Boston, Mass., USA, Sept. 1987, pp. 337-346.

[2] Childs D., Nelson C., Nicks C., Scharrer J., Elrod D., Hale K.: *Theory versus Experiment for the Rotordynamic Coefficients of Annular Gas Seals: Part 1 - Test Facility and Apparatus.* ASME J Tribology, Vol. 108, 1986, pp. 426-432.

[3] Childs D., Scharrer J.: *An Iwatsubo-based Solution for Labyrinth Seals. Comparison to Experimental Results.* J. Eng. for Gas Turbines and Power, Vol. 108, 1986, pp. 599-604.

[4] Hauck L.: *Measurement and Evaluation of Swirl-Tip Flow in Labyrinth Seals of Conventional Turbine Stages.* NASA Conference Publication 2250, 1982, pp. 242-259.

[5] Kwanka K.: *Stability Behavior of a Three Journal Bearing Rotor System Excited by a Lateral Force.* ISROMAC-3, Dynamics (Editor J.H. Kim and W.J. Wang), Honolulu, Hawaii, USA, April 1990, pp. 387-400.

[6] Leie B., Thomas H.-J.: *Self-excited Rotor Whirl Due to Tip-Seal Leakage Forces.* NASA Conference Publication 2133, 1980, pp. 303-316.

[7] Nordmann R., Massmann H.: *Identification of Stiffness, Damping and Mass Coefficients for Annular Seals.* IMechE, Paper C 280/84, 1984, pp. 159-166.

[8] Nordmann, R., Weiser, P.: *Evaluation of Rotordynamic Coefficients of Look- Trough Labyrinth by Means of a Three Bulk Flow Model.* NASA Conference Publication 3122, 1990, pp. 147-163.

[9] Nordmann R., Dietzen, F.: *A 3D Finit-Difference Method for Calculating the Dynamic Coefficients of Seals.* ISROMAC-2, Honolulu, Hawaii, 1988

[10] Ortinger W.: *The Calculation of Friction Factors in a Labyrinth Seal by Means of Turbulent Flow Computation.* ISROMAC - 4, Honolulu, Hawaii, USA, April 1992, pp. 340-349.

[11] Steckel J.: *Experimentelle Untersuchungen zum Durchfluß- und Radialkraftverhalten einer Labyrinthdichtung.* Dissertation TU München, 1993.

[12] Thieleke G., Stetter H.: *Experimental Investigations of Exciting Forces Caused by Flow in Labyrinth Seals.* NASA Conference Publication 3122, 1990, pp. 109-134.